Desalination and Water Treatment
www.deswater.com
doi: 10.1080/19443994.2016.1151379

57 (2016) 25070–25079
November

Taylor & Francis
Taylor & Francis Group

Preparation and characterisation of activated carbon from animal bones and its application for removal of organic micropollutants from aqueous solution

Chahrazed Djilani[a,*], Rachida Zaghdoudi[b,c], Fayçal Djazi[a,c], Bachir Bouchekima[d], Abdelaziz Lallam[e], Pierre Magri[f]

[a]*Faculté de Technologie, Université du 20 Août 1955, B.P 26, Skikda 21000, Algeria, Tel. +213 791 665403; email: chahrazed_dj@yahoo.fr (C. Djilani)*
[b]*Faculté des sciences, Université du 20 Août 1955, B.P 26, Skikda 21000, Algeria, Tel. +213 558 872108*
[c]*Laboratoire LRPCSI, Université du 20 Août 1955, B.P 26, Skikda 21000, Algeria, Tel. +213 771 531297*
[d]*Laboratoire de Développement des Energies Renouvelables (LENREZA), Université Kasdi Merbah, BP 511, Ouargla 30000, Algeria, Tel. +213 773 725299*
[e]*Laboratoire de Physique et Mécanique Textiles de l'ENSISA (LPMT), Université de Haute Alsace, 11 rue Alfred Werner, F 68093, Mulhouse CEDEX, France, Tel. +33 389 336900*
[f]*LCP-A2MC, EA4164, Université de Lorraine, 1bd Arago-57078, Metz, Cedex 3, France, Tel. +33 387 315433*

Received 29 June 2015; Accepted 30 January 2016

ABSTRACT

The present work aimed to investigate the removal feasibility of organic micropollutants (o-nitrophenol (o-NP) and p-nitrotoluene (p-NT)) from aqueous solutions using an original activated carbon prepared from chicken bones (CAB). The activated carbon is treated with 30% H_2O_2 and carbonised at 800°C for 3 h. Thus, the obtained CAB is characterised by the way of different physico-analytical methods as X-ray diffraction, scanning electron microscopy, Fourier transform infrared spectroscopy and the method of Boehm titration. The kinetic experimental data were fitted according to theoretical models: pseudo-first-order, pseudo-second-order, intraparticle diffusion models and the Elovich and Avrami models. The maximum removal obtained for o-NP and p-NT is around ~80% at 5–20 mg/L respectively. The required time for the adsorption equilibrium is between 70 and 145 min. The adsorption kinetics of o-NP and p-NT is tested according to the intraparticle diffusion equations. The results obtained in the present study indicate that the bioadsorbent material CAB is a promising adsorbent for the removal of organic micropollutants from wastewater.

Keywords: Adsorption; Activated carbon; Chicken bones; Industrial wastewater; Organic micropollutant

1. Introduction

Aromatic compounds are major pollutants, as they are usually highly toxic and often carcinogenic. Such compounds are common contaminants in wastewaters [1–3]. Many industrial activities, particularly the textile, paper, plastics, coal, food, petrochemical, pharmaceutical and dye industries, discharge effluents containing various chemicals are toxic to humans and harmful to the environment [4,5].

*Corresponding author.

Several methods such as adsorption, chemical oxidation, photodegradation, coagulation and flocculation are being used for the removal of aromatics compounds from wastewater and particularly the adsorption technology for the removal of organic compounds from wastewaters [1].

Activated carbon adsorption is a widely used technique for the removal of organic and inorganic pollutants from water and gas environments due to their high surface area, porosity and specific surface chemistry. Despite the widespread use of activated carbon in water treatment, the application of the solid adsorbent is limited by the high cost of the material. The literature reveals a developing research interest in establishing the production of activated carbon from low-cost and renewable precursors [6]. Numerous low-cost alternative adsorbents have been proposed, including pomegranate peel [7], algae [8], sawdust [9], chitosan [10], animal bones [11], tree ferns [12], dried plants [13], melon seeds [14], grain sorghum [15] and coir pith [16].

Many studies in the literature are related to the production and characterisation of activated carbon from animal bones [17–24].

Bones consist about 30% by weight of organic compounds, mainly fibrous protein collagen, while the remaining 70% represent inorganic phase composed of defect, poorly crystalline, cation and anion substituted hydroxyapatite Ca_{10} $(PO_4)_6(OH)_2$(HAP) [25].

Animal bones are chosen because of their availability and desirable physical characteristics as activated carbon precursors. Therefore, this study was conducted to investigate the potential of activated carbon from chicken bones (CAB) as an effective adsorbent for the removal of organic micropollutants from industrial wastewater.

2. Materials and methods

2.1. Adsorbent development and characterisation

Chicken bones were collected from a local restaurant in Skikda, Algeria. The results reported in the literature show that animal bones contain mainly Ca and P, with small amounts of Mg, K, Na and other minerals [11,18,25]. All attached meat and fat were removed and cleaned from the bones. Bones were crushed into 1–2-cm pieces and washed with hot distilled water and boiled at least three times in distilled water for 2 h to remove fatty residues. Then, the bones were dried at 80˚C. After drying, bones were treated with an oxidation agent (30% H_2O_2) in order to remove the organic phase of the bone. The H_2O_2 solution was changed daily and heated to its boiling temperature, three times a day. The process was stopped after three days, and the sample was dried at 80˚C during 24 h.

The obtained sample was calcined (in a muffle furnace) for 3 h at 800˚C and grounded to a fine powder using a grinder. Finally, the material was dried in an oven at a temperature of 110˚C for at least 24 h. The activated carbons, thus obtained displayed a pore diameter ranging from 150 to 250 μm.

The morphology, structure and properties of the activated carbon from CAB were determined by X-ray diffraction (XRD), scanning electron microscopy (SEM), Fourier transform infrared spectroscopy (FTIR) and the Boehm titration method.

XRD studies were performed using a Bruker diffractometer, model D8 Advance, equipped with a Cu Kα source and a LynxEyes fast detector (system θ–θ) and operated at the monochromatic radiation $K\alpha_1$ wavelength of copper (λ = 1.5406 Å). The measured angular field ranged from $2\theta = 8^\circ$ to 80° for the CAB.

The microstructure of the adsorbent was observed using a scanning electron microscope (SEM) (Model JEOL JSM 840) operated at a voltage of 7 kV, to generate the flow of secondary electrons necessary for the formation of a surface image.

FTIR was used to detect the functional groups present at the surface of the adsorbent. The spectra were recorded in the frequency range of 650–4,000 cm^{-1} using an FTIR spectrophotometer (Spectrum One FTIR spectrometer).

The concentration of acidic surface oxygen groups (carboxylic, lactonic and phenolic groups) was determined using the Boehm titration method [26]. The Boehm method was performed as follows: 0.5 g of carbon sample was added to a series of flasks containing 50 ml of 0.01 N NaOH, Na_2CO_3, $NaHCO_3$ and HCl solutions. The flasks were then sealed and shaken for 72 h at room temperature. The supernatant solutions were filtered using a Whatman membrane filter with a pore size 0.45 μm, and 10 ml of the remaining solution was titrated with 0.01 N HCl or NaOH, depending on the original solution used. The number of acidic groups was calculated based on the assumptions that NaOH neutralises carboxylic, lactonic and phenolic groups; Na_2CO_3 neutralises carboxylic and lactonic groups; and $NaHCO_3$ neutralises only carboxylic groups. The number of basic sites was determined from the amount of HCl that reacted with the carbon [27].

2.2. Adsorption experiments

Adsorption tests were performed with o-nitrophenol (o-NP) and p-nitrotoluene (p-NT), two micropollutants frequently found in industrial emissions. As usual, an adsorbent material sample with a mass of 0.1 g was placed in a vessel containing 50 mL of an aqueous solution of o-NP or p-NT at an initial concentration of 5 or 20 mg/L, respectively. The experiments were carried out at room temperature while stirring at 250 rpm. The pH values of the aqueous solutions of o-NP and p-NT were respectively, 4.9–5.5. The solution was sampled during the adsorption process, and samples were analysed after filtration through a 0.45-μm RC membrane. Sample concentrations were measured with a Shimadzu UV-1700 spectrophotometer at wavelengths of 273 nm for o-NP and 285 nm for p-NT.

The amount of organic compounds adsorbed per gram of adsorbent (q_t, mg/g) at time (t) was calculated using the following formula:

$$q_t = \frac{(C_i - C_t) \cdot V}{W} \quad (1)$$

where W is the mass of adsorbent expressed in g, V is the volume of the solution in L, C_t (mg/L) is the liquid concentration of organic compounds at any time and C_i (mg/L) is the initial concentration of the organic compounds in solution.

The equilibrium adsorption, q_e (mg/g), was calculated using the following formula:

$$q_e = \frac{(C_i - C_e) \cdot V}{W} \quad (2)$$

where C_i and C_e (mg/L) are the liquid concentrations of the organic compounds initially and at equilibrium, respectively.

$$R(\%) = \frac{C_i - C_e}{C_i} \times 100 \quad (3)$$

where C_i and C_e (mg/L) are the initial and equilibrium concentrations of organic compounds in solution, respectively.

2.3. Adsorption kinetic studies

Pseudo-first-order [28,29], pseudo-second-order [30], intraparticle diffusion [31], Elovich [32] and Avrami [33–35] model kinetic equations are given in Table 1.

3. Results and discussion

3.1. Properties of the activated carbon

XRD was employed to evaluate the phase purity and the crystallographic structural properties of the activated carbon prepared from animal bones (Fig. 1). XRD analysis revealed the crystal structure of CAB. Additionally, in the spectrum of CAB, trace amounts of CaO and MgO were observed and can be ascribed to the decomposition of non-stoichiometric carbonate containing apatite bone [25,36]. For 2θ values, between 25° and 45°, the main lattice reflections peaks are 25°, 28.1°, 32.8°, 33.7°, 34.5° and 39.7° and assigned to the (0 0 2), (1 0 2), (2 1 0), (2 1 1), (1 1 2) and (3 0 0) Miller plans of hydroxyapatite, respectively [18]. Additionally, a peak from $Ca_{10}(PO_4)_6(OH)_2$ appeared [22].

Furthermore, the diffraction patterns of the crystalline form of hydroxyapatite were observed in the X-ray results of CAB. In general, the diffraction pattern of the bioadsorbent is very similar to those reported for other bone chars obtained from swine, animal bone meal and bovine bones [18,25,37].

SEM was employed to observe the surface morphology of CAB. The SEM images (Fig. 2) obtained at different magnifications revealed the irregular morphology of CAB. The surface of CAB is heterogeneous. The structural heterogeneity is a result of existence of micropores, mesopores and macropores of different sizes and shapes [38] and, in our CAB, the presence of mesopores and macropores. The presence of mesopores is also valuable for the adsorption of large molecules or when a faster adsorption rate is required [39].

The FTIR spectrum of CAB is shown in Fig. 3. The absorption peak at 3,695.63 cm^{-1} indicates the presence of OH groups, which can be attributed to adsorbed water on the carbon. The peaks at 1,024.58, 1,086.44 and 962.45 cm^{-1} arose from the different vibrational modes of the $-PO_4^{3-}$ groups. The band in the 900–800 cm^{-1} region may be attributed to symmetric CO_3^{2-} stretching and is associated with the deformation of the carbonate group [11,25,40,41].

The small bands at 1,462.16 cm^{-1} confirm the above-mentioned existence of carbonate groups in the natural hydroxyapatite. The band at approximately 869.83 cm^{-1} confirms HPO_4^{2-} [41]. In the region of 2,014.79–2,299.84 cm^{-1}, overtones and combinations of the $-PO_4^{2-}$ are observed [25].

A large number of bands in the spectra (3,695.63, 1,462.16, 1,086.44, 1,024.58, 962.45 and 869.83 cm^{-1}) are in agreement with the literature data on hydroxyapatite [39,42,43].

The presence of different oxygen-containing functional groups on the surface of activated carbon is a

Table 1
Names and non-linear forms of studied kinetic models

$\log(q_e - q_t) = \log q_e - \frac{k_1}{2{,}303} \times t$	Pseudo-first-order
$\Delta q(\%) = 100\sqrt{\frac{\sum[(q_{exp}-q_{cal})/q_{exp}]^2}{N-1}}$	Normalized standard deviation
$\frac{t}{q_t} = \frac{1}{k_2 q_e^2} + \frac{1}{q_e} t$	Pseudo-second-order
$q_t = k_{int} t^{1/2}$	Intraparticle diffusion
$q_t = \frac{1}{\beta}\ln(\alpha\beta) + \frac{1}{\beta}\ln t$	Elovich
$\ln(-\ln(1-\alpha)) = n_{AV}\ln k_{AV} + n_{AV}\ln t$	Avrami

Notes: k_1: rate constant for the pseudo-first-order adsorption; k_2: rate constant for the pseudo-second-order adsorption; N: is the number of data points, q_{exp} and q_{cal} are the experimental and calculated adsorption capacity value; k_{AV}, n_{AV}: Avrami constants; α, β: Elovich constants; k_{int}: intraparticle diffusion constant.

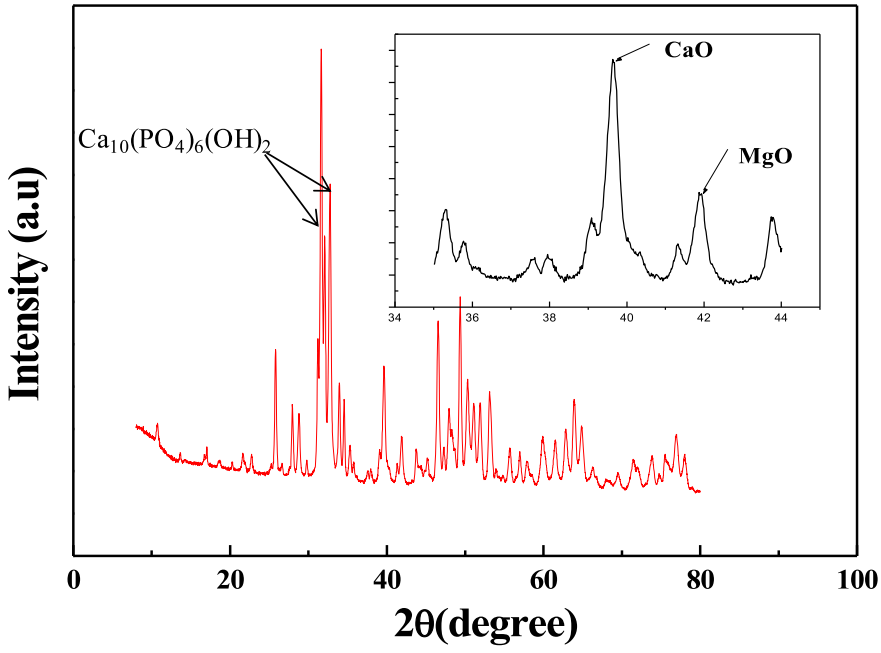

Fig. 1. XRD pattern of CAB.

very important characteristic because, these groups have a strong effect on the adsorption properties of the activated carbon. The results of the identification and quantification of the oxygen groups in the prepared carbon are shown in Table 2. The functional groups at the surface of the CAB, characterised by the Boehm method, were predominantly basic (0.760 meq/$g_{sorbent}$), which is in a good agreement with the pH value, followed by lactonic (0.090 meq/$g_{sorbent}$), phenolic (0.076 meq/$g_{sorbent}$) and carboxylic (0.070 meq/$g_{sorbent}$) groups.

It should be mentioned that this distribution of different oxygen groups is logical because pyrolysis at high temperature leads to the formation of activated carbons with a basic surface. The number of acid functional groups is very low and approximate, because the Boehm method is an approximate method.

3.2. Adsorption kinetic studies

Fig. 4 demonstrates the effect of contact time on the adsorption of o-NP by CAB for initial concentrations of 5–20 mg/L. The adsorption process was highly rapid within the first few minutes (contributing to external surface adsorption), regardless of the concentration, and it gradually slowed down as equilibrium was approached (contributing to internal surface adsorption). A similar phenomenon was observed for

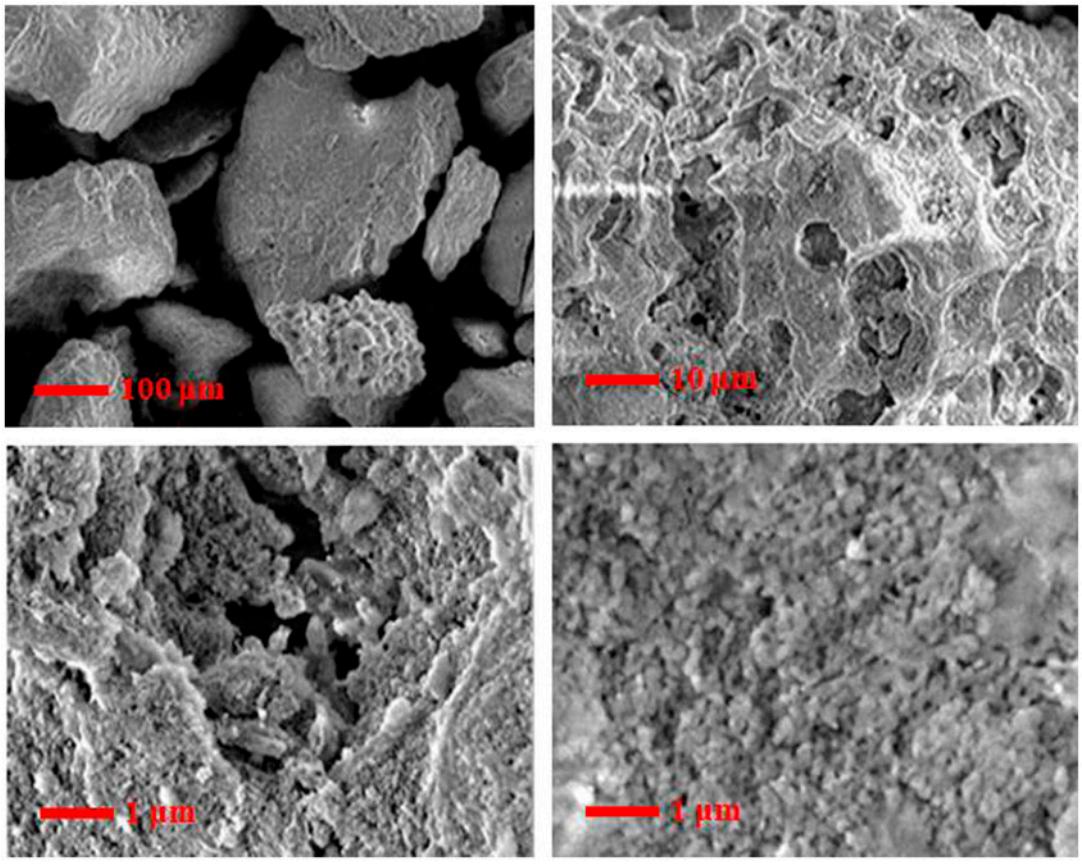

Fig. 2. SEM of CAB at different magnifications.

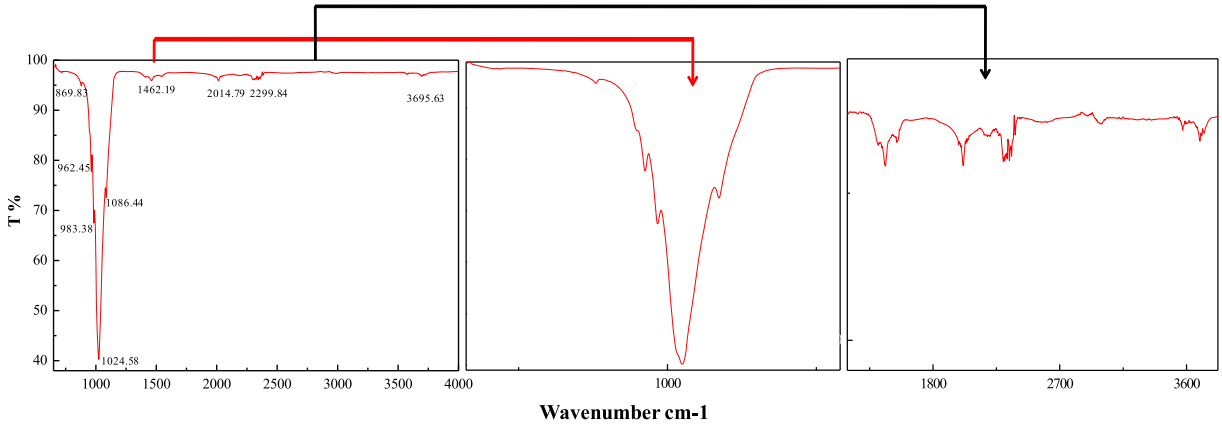

Fig. 3. FTIR spectrum of CAB.

the adsorption of p-NT (Fig. 5). The phenomenon may be observed because, initially, all active sites on the adsorbents surface were vacant and because of the high concentration of the solution. After that period, few surface active sites were available; therefore, only a very small increase in the o-NP and p-NT uptake was observed [44]. However, there was a reverse relationship between the adsorptive removal efficiency of o-NP, R (%) and the initial concentration. The maximum R (%) values at the initial concentrations of 5–20 mg/L for o-NP were observed to be 77% (1.6836 mg/g) and 68% (6.875 mg/g), respectively,

Table 2
Surface chemistry of activated carbon prepared from animal bones

Properties (meq/g)	CAB
pH	8.38
Carboxylic groups	0.070
Lactonic groups	0.090
Phenolic groups	0.076
Acid groups	0.236
Basic groups	0.760
Total	0.996

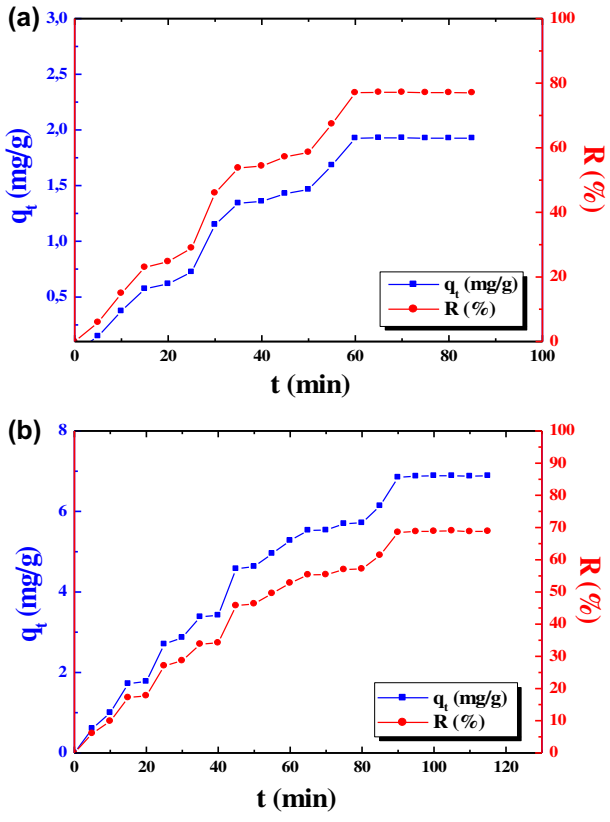

Fig. 4. Adsorption of o-NP on bioadsorbent prepared from CAB: (a) [o-NP] = 5 mg/L and (b) [o-NP] = 20 mg/L.

which may be due to the saturation of adsorption sites at higher o-NP concentrations. The percentage removal of p-NT was 78% (1.915 mg/g) at an initial concentration of 5 mg/L and 80% (7.335 mg/g) at an initial concentration of 20 mg/L. A comparative analysis showed that the CAB was efficient in removing organic micropollutants (Table 3).

Pseudo-first- and second-order kinetics models, an intraparticle diffusion model and the Elovich and Avrami models were used to examine the mechanism

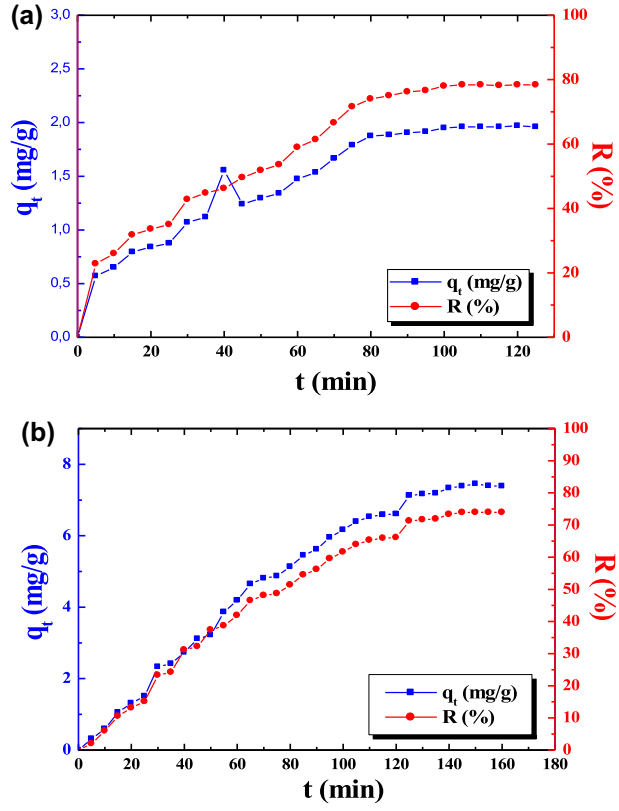

Fig. 5. Adsorption of p-NT on bioadsorbent prepared from CAB: (a) [p-NT] = 5 mg/L and (b) [p-NT] = 20 mg/L.

controlling the adsorption process, such as a chemical reaction, diffusion control or mass transfer.

Several formalisms have been established in the literature to describe the kinetics of absorption. In this study, we used the first- and second-order kinetic laws. The rate constant for the first-order adsorption is derived from the model established by Lagergren. The selected models are simple and are well suited to describe the adsorption kinetics of organic compounds [14].

The constants of the kinetics models for the adsorption of o-NP and p-NT by CAB are listed in Table 4. It can be concluded that the pseudo-first-and second-order equations do not give a good fit to the experimental data for the adsorption of o-NP and p-NT.

An intraparticle diffusion model based on the theory proposed by Weber and Morris was tested to identify the diffusion mechanism. It is an empirically found functional relationship, common to most adsorption processes, in which the uptake varies almost proportionally with $t^{1/2}$ rather than with the contact time t (Table 1) [45].

Table 3
Comparison percentage removal of various adsorbents for o-NP and p-NT

	Percentage removal				
	o-NP initial concentration		p-NT initial concentration		
Precursor	5 mg/L	20 mg/L	5 mg/L	20 mg/L	Refs.
Coffee grounds	80.6	88	95.4	97.4	[14]
Melon seeds	80.8	78.15	89.8	99.4	[14]
Orange peels	80.5	89.9	96.6	95.25	[14]
Chicken bones	77	68	78	80	Present study

Table 4
Kinetic parameters

	o-NP initial concentration (mg/L)		p-NT initial concentration (mg/L)	
Kinetic parameter	5	20	5	20
Pseudo-first-order				
k_1 (min^{-1})	0.0368	0.0479	0.0419	0.0279
q_{exp}	1.6836	6.8750	1.9150	7.3350
q_{cal}	2.4038	16.4437	3.2299	13.7911
Δq (%)	13.53	32.80	35.20	93.84
R^2	0.9716	0.8073	0.8938	0.9274
Pseudo-second-order				
k_2 (g mg^{-1} min^{-1}) × 10^{-3}	3.9946	0.0811	8.7526	0.2063
q_{cal}	3.5574	34.2466	2.6882	20.2020
Δq (%)	16.18	16.94	9.52	33.76
R^2	0.5511	0.1784	0.9590	0.4883
Intraparticle diffusion				
k_{int} (mg g^{-1} $min^{-1/2}$)	0.2880	0.8653	0.1835	0.7479
R^2	0.9807	0.9923	0.9816	0.9857
Elovich				
α (mg g^{-1} min^{-1})	0.1215	0.3517	0.2299	0.3723
β (g mg^{-1})	1.3342	0.4222	2.1510	0.5228
R^2	0.9674	0.9656	0.9532	0.9025
Avrami				
n_{AV}	1.3077	1.2976	0.8918	1.4022
k_{AV} (min^{-1})	0.0285	0.024	0.039	0.0162
R^2	0.9878	0.9602	0.9210	0.9882

If the Weber–Morris plot of q_t vs. $t^{1/2}$ satisfies the linear relationship with the experimental data, then the sorption process is found to be controlled only by intraparticle diffusion. The intraparticle diffusion model may present multi-linearity, which indicates that two or more steps occur in the adsorption processes [46]. The first, sharper portion is the external surface adsorption or instantaneous adsorption stage. The second portion is the gradual adsorption stage, where the intraparticle diffusion is rate controlled. The third portion is the final equilibrium stage, where the intraparticle diffusion starts to slow down due to the extremely low solute concentration in solution [47].

The rate of uptake might be limited by the size of adsorbate molecule, concentration of the adsorbate, affinity to the adsorbent, diffusion coefficient of the adsorbate in the bulk phase, pore size distribution of the adsorbent and degree of mixing. The intraparticle diffusion is generally the rate-limiting step for systems with high concentrations of adsorbate, good mixing, large particle sizes and low affinity towards the adsorbent [48].

The plots are not linear over the entire time range (Figure not shown), implying that more than one process is controlling the sorption process. If the two steps are independent of one another, the plot of q_t vs. $t^{1/2}$ appears as a combination of two or more intersecting lines. The intraparticle diffusion equation provides the best correlation coefficient, and the value of k_{int} increased as the initial organic micropollutants concentration increased (5–20 mg/L). The high values of R^2 (Table 4) indicate the possibility of the sorption process to be controlled by both particle and pore diffusion [49]. Additionally, the C values (–0.5215, –1.6596 for o-NP and 0.0776, –1.5544 for p-NT) decreased as their concentrations increased from 5 to 20 mg/L.

The intraparticle diffusion of CAB is likely to occur in three stages. The adsorbate molecule rapidly enters the macropores and wider mesopores and then penetrates more slowly into the smaller mesopores. The linear portion of the plot for a wide range of contact times between the adsorbent and adsorbate does not pass through the origin. This deviation from the origin or near the saturation point may be due to the differences in the rates of mass transfer in the initial and final stages of adsorption. Furthermore, such deviation from the origin indicates that the pore diffusion is not the only rate controlling step.

The Elovich equation has been successfully applied to represent chemisorption processes at low adsorption rates. The same equation was used to model the adsorption on heterogeneous surfaces. The Elovich rate equation uses constants for adsorption and desorption to describe the kinetics of chemisorption on highly heterogeneous surfaces. The experimental data in this study do not show a good fit to this equation, as they do to the intraparticle diffusion equation. However, the results obtained by applying this model to the adsorption of o-NP and p-NT on CAB show acceptable correlation coefficients, with the lowest being $R^2 = 0.9025$ for p-NT (20 mg/L).

The Avrami exponential is a fractional number related to the possible changes in the adsorption mechanism that occur during the adsorption process. Therefore, the adsorption mechanism model may take into account a change in the kinetic order which occur during the contact of the adsorbate with the adsorbent [14]. The corresponding Avrami parameters, along with the correlation coefficients, are shown in Table 4. The regression values determine the suitability of this model.

The validity of the abovementioned kinetic models for o-NP and p-NT adsorption on CAB ranked as follows: intraparticle > Avrami > Elovich > pseudo-first-order > pseudo-second-order.

4. Conclusions

The present investigation demonstrated that CAB can be effectively used as a raw material for the preparation of activated carbon for the removal of organic micropollutants from aqueous solution. Animal bone is a low-cost waste residue that is easily available in large quantities. The activated carbon was characterised and has been used for the removal of o-NP and p-NT from aqueous solution. Characterisation studies performed via XRD and FTIR, ascertained that the activated carbon prepared from animal bones was rich in calcium. The majority of the functional groups in the activated carbon were basic according to both pH and titration measurements. The percentage of organic micropollutant removal by CAB was 77% for o-NP and 78% for p-NT, at an initial concentration of 5 mg/L and 68% for o-NP and 80% for p-NT at an initial concentration of 20 mg/L. A comparative analysis indicated that the activated carbon is efficient in removing organic micropollutants. The kinetics data were analysed using five adsorption kinetic models: pseudo-first- and second-order equations, an intraparticle diffusion equation and the Elovich and Avrami equations. The results indicate that the intraparticle diffusion equation fits the experimental data notably well, and it is demonstrated that CAB can be an alternative source for low-cost absorbents.

References

[1] P.A. Mangrulkar, S.P. Kamble, J. Meshram, S.S. Rayalu, Adsorption of phenol and o-chlorophenol by mesoporous MCM-41, J. Hazard. Mater. 160 (2008) 414–421.
[2] S.P. Kamble, P.A. Mangrulkar, A.K. Bansiwal, S.S. Rayalu, Adsorption of phenol and o-chlorophenol on surface altered fly ash based molecular sieves, Chem. Eng. J. 138 (2008) 73–83.
[3] F. Villacañas, M.F.R. Pereira, J.J.M. Órfão, J.L. Figueiredo, Adsorption of simple aromatic compounds on activated carbons, J. Colloid Interface Sci. 293 (2006) 128–136.
[4] T.A. Özbelge, Ö.H. Özbelge, S.Z. Başkaya, Removal of phenolic compounds from rubber–textile wastewaters by physico-chemical methods, Chem. Eng. Process. Process Intensif. 41 (2002) 719–730.
[5] S. Dutta, J.K. Basu, R.N. Ghar, Studies on adsorption of p-nitrophenol on charred saw-dust, Sep. Purif. Technol. 21 (2001) 227–235.
[6] V.O. Njoku, K.Y. Foo, B.H. Hameed, Microwave-assisted preparation of pumpkin seed hull activated carbon and its application for the adsorptive removal of 2,4-dichlorophenoxyacetic acid, Chem. Eng. J. 215–216 (2013) 383–388.
[7] E.-S.Z. El-Ashtoukhy, N.K. Amin, O. Abdelwahab, Removal of lead (II) and copper (II) from aqueous solution using pomegranate peel as a new adsorbent, Desalination 223 (2008) 162–173.
[8] S. Altenor, M.C. Ncibi, E. Emmanuel, S. Gaspard, Textural characteristics, physiochemical properties and adsorption efficiencies of Caribbean alga Turbinaria turbinata and its derived carbonaceous materials for water treatment application, Biochem. Eng. J. 67 (2012) 35–44.
[9] K.G. Sreejalekshmi, K. Anoop Krishnan, T.S. Anirudhan, Adsorption of Pb(II) and Pb(II)-citric acid on sawdust activated carbon: Kinetic and equilibrium isotherm studies, J. Hazard. Mater. 161 (2009) 1506–1513.
[10] R. Laus, T.G. Costa, B. Szpoganicz, V.T. Fávere, Adsorption and desorption of Cu(II), Cd(II) and Pb(II) ions using chitosan crosslinked with epichlorohydrin-triphosphate as the adsorbent, J. Hazard. Mater. 183 (2010) 233–241.
[11] B. Kizilkaya, A.A. Tekinay, Y. Dilgin, Adsorption and removal of Cu(II) ions from aqueous solution using pretreated fish bones, Desalination 264 (2010) 37–47.
[12] Y.-S. Ho, Removal of metal ions from sodium arsenate solution using tree fern, Process Saf. Environ. Prot. 81 (2003) 352–356.
[13] M. Chiban, A. Soudani, F. Sinan, M. Persin, Wastewater treatment by batch adsorption method onto microparticles of dried Withania frutescens plant as a new adsorbent, J. Environ. Manage. 95 (2012) S61–S65.
[14] C. Djilani, R. Zaghdoudi, A. Modarressi, M. Rogalski, F. Djazi, A. Lallam, Elimination of organic micropollutants by adsorption on activated carbon prepared

from agricultural waste, Chem. Eng. J. 189–190 (2012) 203–212.
[15] Y. Diao, W.P. Walawender, L.T. Fan, Activated carbons prepared from phosphoric acid activation of grain sorghum, Bioresour. Technol. 81 (2002) 45–52.
[16] C. Namasivayam, D. Sangeetha, Removal of molybdate from water by adsorption onto $ZnCl_2$ activated coir pith carbon, Bioresour. Technol. 97 (2006) 1194–1200.
[17] S. Al-Asheh, N. Abdel-Jabar, F. Banat, Packed-bed sorption of copper using spent animal bones: Factorial experimental design, desorption and column regeneration, Adv. Environ. Res. 6 (2002) 221–227.
[18] M. El Haddad, R. Mamouni, N. Saffaj, S. Lazar, Removal of a cationic dye—Basic red 12—From aqueous solution by adsorption onto animal bone meal, JAAUBAS 12 (2012) 48–54.
[19] I. Smičiklas, S. Dimović, I. Plećaš, M. Mitrić, Removal of Co^{2+} from aqueous solutions by hydroxyapatite, Water Res. 40 (2006) 2267–2274.
[20] F. Banat, S. Al-Asheh, F. Mohai, Batch zinc removal from aqueous solution using dried animal bones, Sep. Purif. Technol. 21 (2000) 155–164.
[21] W. Huang, H. Zhang, Y. Huang, W. Wang, S. Wei, Hierarchical porous carbon obtained from animal bone and evaluation in electric double-layer capacitors, Carbon 49 (2011) 838–843.
[22] X. Pan, J. Wang, D. Zhang, Sorption of cobalt to bone char: Kinetics, competitive sorption and mechanism, Desalination 249 (2009) 609–614.
[23] R. Leyva-Ramos, J. Rivera-Utrilla, N.A. Medellin-Castillo, M. Sanchez-Polo, Kinetic modeling of fluoride adsorption from aqueous solution onto bone char, Chem. Eng. J. 158 (2010) 458–467.
[24] H. Modin, K.M. Persson, A. Andersson, M. van Praagh, Removal of metals from landfill leachate by sorption to activated carbon, bone meal and iron fines, J. Hazard. Mater. 189 (2011) 749–754.
[25] S. Dimović, I. Smičiklas, I. Plećaš, D. Antonović, M. Mitrić, Comparative study of differently treated animal bones for Co^{2+} removal, J. Hazard. Mater. 164 (2009) 279–287.
[26] H.P. Boehm, Surface oxides on carbon and their analysis: A critical assessment, Carbon 40 (2002) 145–149.
[27] D. Prahas, Y. Kartika, N. Indraswati, S. Ismadji, Activated carbon from jackfruit peel waste by H_3PO_4 chemical activation: Pore structure and surface chemistry characterization, Chem. Eng. J. 140 (2008) 32–42.
[28] C. Escudero, C. Gabaldon, P. Marzal, I. Villaescusa, Effect of EDTA on divalent metal adsorption onto grape stalk and exhausted coffee wastes, J. Hazard. Mater. 152 (2008) 476–485.
[29] O.P. Junior, A.L. Cazetta, R.C. Gomes, É.O. Barizão, I.P.A.F. Souza, A.C. Martins, T. Asefa, V.C. Almeida, Synthesis of $ZnCl_2$-activated carbon from macadamia nut endocarp (*Macadamia integrifolia*) by microwave-assisted pyrolysis: Optimization using RSM and methylene blue adsorption, J. Anal. Appl. Pyrolysis 105 (2014) 166–176.
[30] N. Azouaou, Z. Sadaoui, A. Djaafri, H. Mokaddem, Adsorption of cadmium from aqueous solution onto untreated coffee grounds: Equilibrium, kinetics and thermodynamics, J. Hazard. Mater. 184 (2010) 126–134.
[31] S. Liang, X. Guo, N. Feng, Q. Tian, Isotherms, kinetics and thermodynamic studies of adsorption of Cu^{2+} from aqueous solutions by Mg^{2+}/K^{+} type orange peel adsorbents, J. Hazard. Mater. 174 (2010) 756–762.
[32] A.B. Perez-Marin, V. Meseguer Zapata, J.F. Ortu˜no, M. Aguilar, J. Saez, M. Llorens, Removal of cadmium from aqueous solutions by adsorption onto orange waste, J. Hazard. Mater. B 139 (2007) 122–131.
[33] A.M.M. Vargas, A.L. Cazetta, M.H. Kunita, T.L. Silva, V.C. Almeida, Adsorption of methylene blue on activated carbon produced from flamboyant pods (Delonix regia): Study of adsorption isotherms and kinetic models, Chem. Eng. J. 168 (2011) 722–730.
[34] D.S.F. Gay, T.H.M. Fernandes, C.V. Amavisca, N.F. Cardoso, E.V. Benvenutti, T.M.H. Costa, E.C. Lima, Silica grafted with a silsesquioxane containing the positively charged 1,4 diazoniabicyclo[2.2.2]octane group used as adsorbent for anionic dye removal, Desalination 258 (2010) 128–135.
[35] A.R. Cestari, E.F.S. Vieira, J.D.S. Matos, D.S.C. dos Anjos, Determination of kinetic parameters of Cu(II) interaction with chemically modified thin chitosan membranes, J. Colloid Interface Sci. 285 (2005) 288–295.
[36] K.D. Rogers, P. Daniels, An X-ray diffraction study of the effects of heat treatment on bone mineral microstructure, Biomaterials 23 (2002) 2577–2585.
[37] R. Tovar-Gómez, M.R. Moreno-Virgen, J.A. Dena-Aguilar, V. Hernández-Montoya, A. Bonilla-Petriciolet, M.A. Montes-Morán, Modeling of fixed-bed adsorption of fluoride on bone char using a hybrid neural network approach, Chem. Eng. J. 228 (2013) 1098–1109.
[38] A.A. Ahmad, B.H. Hameed, A.L. Ahmad, Removal of disperse dye from aqueous solution using waste-derived activated carbon: Optimization study, J. Hazard. Mater. 170 (2009) 612–619.
[39] R.H. Hesas, W.M.A. Wan Daud, J.N. Sahu, A. Arami-Niya, The effects of a microwave heating method on the production of activated carbon from agricultural waste: A review, J. Anal. Appl. Pyrolysis 100 (2013) 1–11.
[40] R. Murugan, S. Ramakrishna, K. Panduranga Rao, Nanoporous hydroxy-carbonate apatite scaffold made of natural bone, Mater. Lett. 60 (2006) 2844–2847.
[41] I. Smičiklas, A. Onjia, S. Raičević, Experimental design approach in the synthesis of hydroxyapatite by neutralization method, Sep. Purif. Technol. 44 (2005) 97–102.
[42] C.Y. Ooi, M. Hamdi, S. Ramesh, Properties of hydroxyapatite produced by annealing of bovine bone, Ceram. Int. 33 (2007) 1171–1177.
[43] K. Haberko, M.M. Bućko, J. Brzezińska-Miecznik, M. Haberko, W. Mozgawa, T. Panz, A. Pyda, J. Zarębski, Natural hydroxyapatite—Its behaviour during heat treatment, J. Eur. Ceram. Soc. 26 (2006) 537–542.
[44] J.Q. Albarelli, R.B. Rabelo, D.T. Santos, M.M. Beppu, M.A.A. Meireles, Effects of supercritical carbon dioxide on waste banana peels for heavy metal removal, J. Supercrit. Fluids 58 (2011) 343–351.
[45] I.A.W. Tan, A.L. Ahmad, B.H. Hameed, Adsorption of basic dye on high-surface-area activated carbon prepared from coconut husk: Equilibrium, kinetic and thermodynamic studies, J. Hazard. Mater. 154 (2008) 337–346.

[46] B.H. Hameed, F.B.M. Daud, Adsorption studies of basic dye on activated carbon derived from agricultural waste: Hevea brasiliensis seed coat, Chem. Eng. J. 139 (2008) 48–55.
[47] M.S. Chiou, G.S. Chuang, Competitive adsorption of dye metanil yellow and RB15 in acid solutions on chemically cross-linked chitosan beads, Chemosphere 62 (2006) 731–740.
[48] M. Uğurlu, A. Gürses, M. Açıkyıldız, Comparison of textile dyeing effluent adsorption on commercial activated carbon and activated carbon prepared from olive stone by $ZnCl_2$ activation, Microporous Mesoporous Mater. 111 (2008) 228–235.
[49] D. Borah, S. Satokawa, S. Kato, T. Kojima, Sorption of As (V) from aqueous solution using acid modified carbon black, J. Hazard. Mater. 162 (2009) 1269–1277.